*Clays and Clay Minerals*, Vol. 35, No. 4, 281–290, 1987.

# KAOLINITE, OPAL-CT, AND CLINOPTILOLITE IN ALTERED TUFFS INTERBEDDED WITH LIGNITE IN THE JACKSON GROUP, TEXAS

A. L. SENKAYI, D. W. MING, J. B. DIXON, AND L. R. HOSSNER

Department of Soil and Crop Sciences, Texas Agricultural Experiment Station
Texas A&M University, College Station, Texas 77843

**Abstract**—The mineralogy of partially kaolinized strata interbedded with lignite at the San Miguel mine, Atascosa County, Texas, was investigated by X-ray powder diffraction and optical and scanning electron microscopy. The San Miguel lignite occurs in the lower Jackson Group (late Eocene) of southern Texas. Based on mineralogical and micromorphological data, some of these clay partings are probably volcanic in origin and were exposed to variable degrees of *in situ* kaolinization in a swamp environment. Coexistence of kaolinite, clinoptilolite, and opal-CT in several of these strata suggests that the partially kaolinized volcanic layers were subjected to a subsequent resilication process following burial. Kaolinite is the dominant mineral in the oldest and most kaolinized volcanic layer (underclay) below the lowest lignite bed (seam D). The kaolinite exhibits a well-developed vermicular morphology. The youngest volcanic layer, which occurs stratigraphically above the uppermost lignite seam, is characterized by pseudomorphs of volcanic glass shards and consists mainly of clinoptilolite. Movement of siliceous ground water from this layer to the underlying strata apparently provided silica-rich solutions from which opal-CT and large (as long as 300 $\mu$m) euhedral crystals of clinoptilolite precipitated in the fossilized plant roots, veinlets, and fractures within the underlying strata. Micromorphological relationships between the Si-rich (opal-CT and clinoptilolite) and sulfide (marcasite and pyrite) minerals in the fossil roots and fractures suggest that the marcasite formed before and pyrite after the resilication process.

**Key Words**—Clinoptilolite, Kaolinite, Lignite, Marcasite, Opal-CT, Plant roots, Pyrite, Silication, Zeolite.

## INTRODUCTION

The mineralogy of partially altered volcanic strata interbedded with coal and lignite has been related to the intensity of weathering and leaching within an acid-swamp environment in which the volcanic materials were deposited. Pevear *et al.* (1980) reported that smectite and cristobalite (with and without clinoptilolite) are the initial alteration products of volcanic materials in many such geologic environments. Reynolds and Anderson (1967) suggested that the high Al/Si ratio of montmorillonite requires that the excess Si be liberated during the transformation of Si-rich tephra to montmorillonite. The Si released by the alteration process may be incorporated in cristobalite or clinoptilolite (Henderson *et al.*, 1971; Reynolds, 1970). Grim and Güven (1978) reported that the formation of clinoptilolite appears to be favored by alkaline conditions and a low intensity of leaching. With more intense leaching and weathering, kaolinite is commonly the stable mineral phase.

In Texas, lignite occurs mainly in three Tertiary geologic units (the Wilcox Group, Yegua Formation, and Jackson Group shown in Figure 1). The lignites in the latter two units are commonly interbedded with volcanic strata, similar to those described by Senkayi *et al.* (1984). Some of the strata or clay partings interbedded with lignite in the lower Jackson Group (late Eocene) at the San Miguel mine in Atascosa County (Figure 1) appear to be volcanic in origin and contain kaolinite, which represents an advanced stage of weathering, as well as clinoptilolite and opal-CT, which are believed to have formed under slightly alkaline conditions (Grim and Güven, 1978). The paragenetic relationships of the apparently metastable mineral assemblage of kaolinite, opal-CT, and clinoptilolite in these strata is the focus of the present paper. Similar clay partings have also been observed in the lower Manning Formation (Jackson Group) lignite at the Gibbons Creek mine in Grimes County (Figure 1), although these are not discussed here in detail.

## ENVIRONMENT OF DEPOSITION

The stratigraphy and environment of deposition of the San Miguel lignite deposit were discussed by Snedden (1979) and McNulty (1978); the following is a summary of their work. Both the lignite and associated strata at the San Miguel mine belong stratigraphically to the lower Jackson Group of southern Texas, which is composed principally of interbedded sands and fossiliferous shales, with abundant volcanic ash and silicified wood (Snedden, 1979). These sediments are part of the south Texas lagoonal-coastal plain system. Numerous volcanic fragments occur in the sediments stratigraphically below and above the lignite (Snedden, 1979). The lignite interval represents a coastal swamp or marsh depositional environment which existed in south Texas during the late Eocene Epoch. The numerous root structures in the underclay and the strata

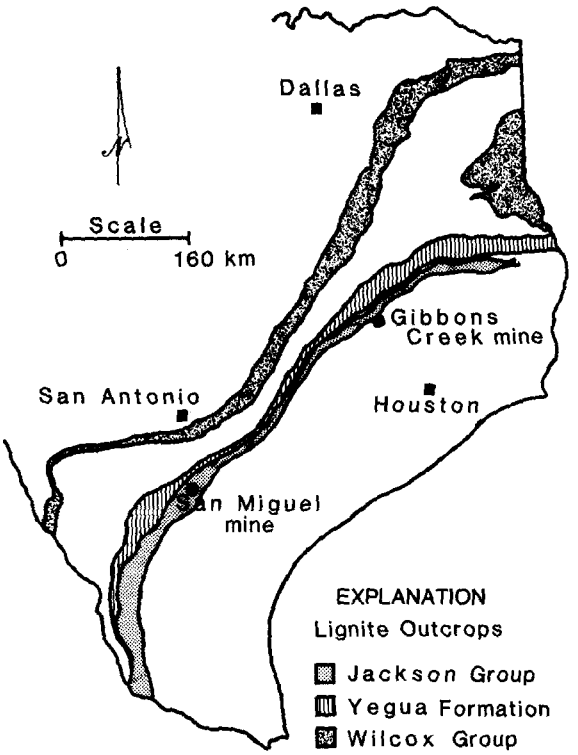


Figure 1. Map showing the location of the sampling site at San Miguel mine, Atascosa County, Texas, and the major geologic units containing lignite (after Kaiser, 1985).

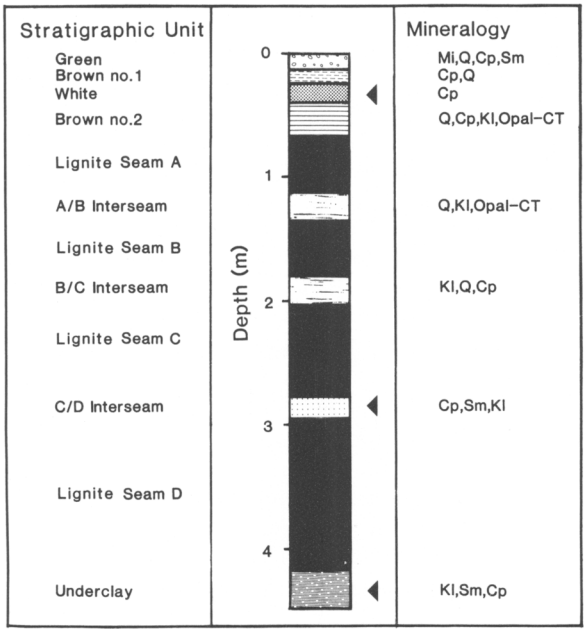


Figure 2. Lithologic column showing mineralogical compositions of the volcanic (indicated by arrows) and other strata investigated. Minerals are listed in decreasing order of relative abundance estimated from X-ray powder diffraction peak intensities. Mi = mica, Q = quartz, Cp = clinoptilolite, Sm = smectite, Kl = kaolinite.

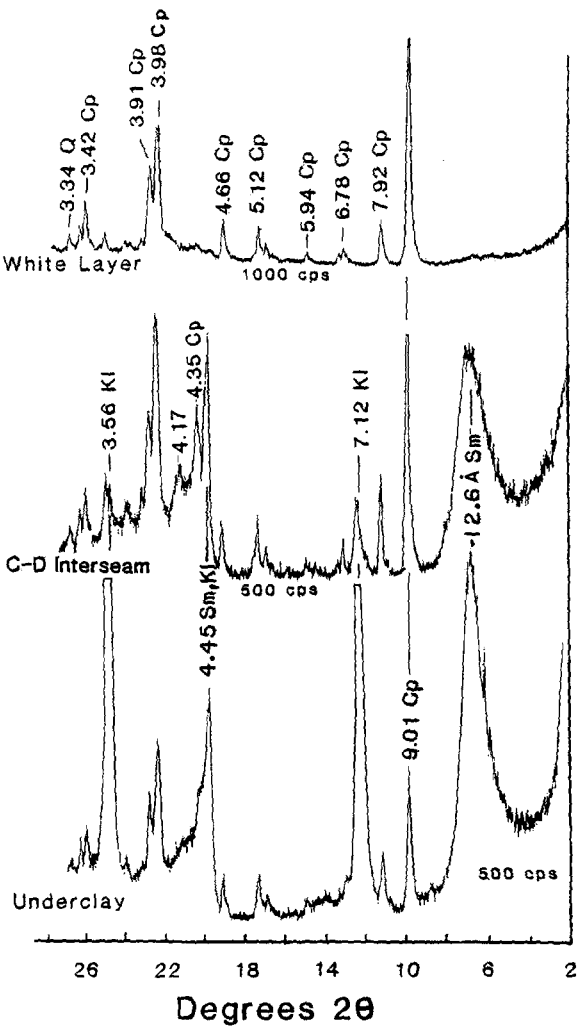


Figure 3. X-ray powder diffraction patterns showing relative distributions of kaolinite, smectite, and clinoptilolite in the volcanic strata shown in Figure 2. Kl = kaolinite, Sm = smectite, Cp = clinoptilolite, Q = quartz.

interbedded with the lignite seams suggest *in situ* formation of the lignite. According to Snedden (1979), the faint but continuous parallel laminations in the lignite indicate that the organic matter accumulated on a dry and plant-covered surface. Vertical and horizontal desiccation fractures are abundant within the lignite seams and associated strata.

The lignite seams are interbedded with several clay partings or layers. According to McNulty (1978), the major clay partings are laterally continuous and have been correlated across the entire length of the lignite deposit (more than 40 km). Snedden (1979) suggested that these clay partings represent splay deposits, although he admitted that splay deposits generally are much more localized than the strata observed here. According to Snedden, periodic flooding following dry

https://doi.org/10.1346/CCMN.1987.0350405 Published online by Cambridge University Press

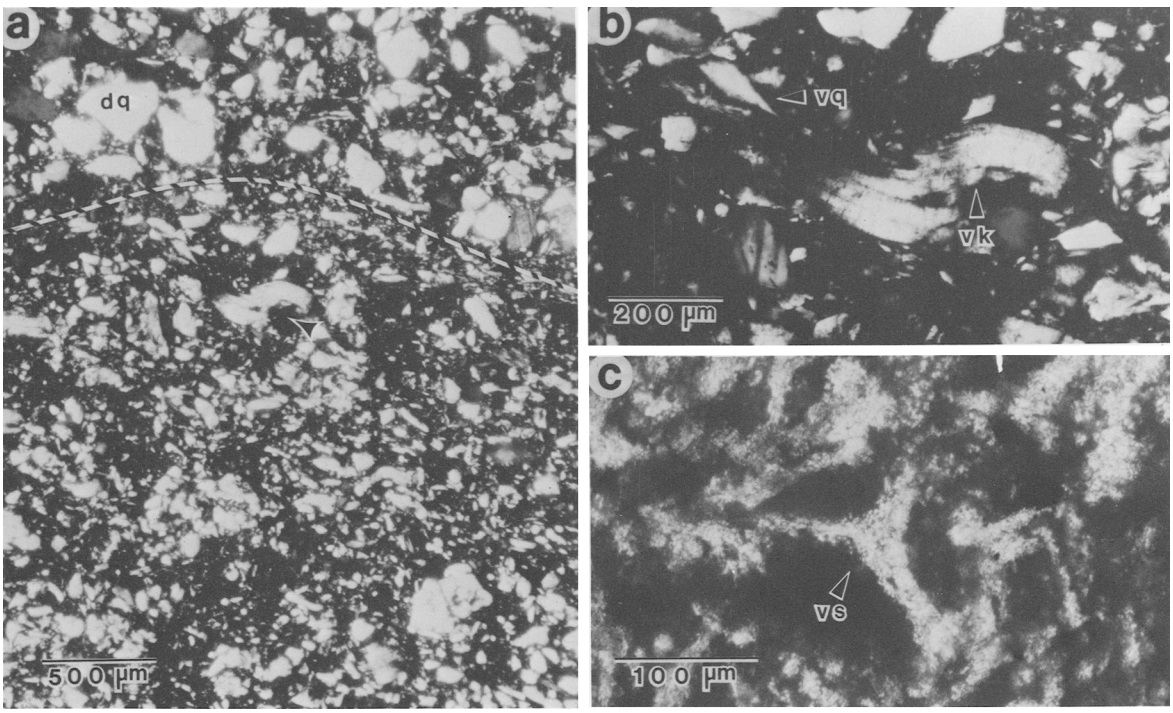


Figure 4. Photomicrographs (plane polarized light) showing: (a) boundary between kaolinized volcanic tuff (below the dotted line) and the overlying non-volcanic material containing large subrounded quartz (dq) grains; (b) vermicular kaolinite (vk) and angular, much smaller volcanic quartz (vq) grains in the area indicated by the arrow in (a), and (c) pseudomorph of volcanic glass shard (vs) in the white volcanic layer (Figure 2). Specimen shown in (a) and (b) is from the B/C interseam (Figure 2).

periods spread thin sheets of clay over the swamp, interrupting the accumulation of organic materials in the swamp. Based on mineralogic and micromorphologic data discussed in this paper, we propose a volcanic origin (i.e., ash falls) for some of these strata. Such an origin explains their great lateral extent, uniformity in thickness, and mineralogical composition.

## MATERIALS AND METHODS

Samples of lignite, the associated overburden and underclay, and the strata interbedded with the lignite seams were collected from a freshly exposed highwall at the San Miguel mine in Atascosa County (Figure 1). The strata sampled were about 50 m below the surface, and the highwall had been exposed for one week. Representative samples were collected from each of the recognizable layers shown in Figure 2. The samples were immediately placed in plastic bags and transported to the laboratory where they were freeze dried and any special features and mineral segregations noted and described. Fossilized roots and veinlets of clinoptilolite from fractures and joints were hand picked from several of the lignite and other layers indicated in Figure 2 for further characterization by X-ray powder diffraction (XRD) and scanning electron microscopy (SEM).

Epoxy-impregnated thin sections of representative bulk specimens, fossil roots, and veinlets of clinoptilolite were prepared for optical microscopy and elemental dot mapping by electron microprobe using a JEOL JSM 35CF microscope. The Si/Al ratios of several zeolite crystals were determined as described by Ming and Dixon (1986). A JEOL JSM-35CF scanning electron microscope equipped with energy- and wavelength-dispersive systems interfaced with a Tracor Northern 1000 microcomputer was used. Al and Si contents were obtained by comparing the intensities of the Al and Si signals from the specimen being analyzed to those from a standard clinoptilolite of known chemical composition. Specimens for the SEM analysis were cemented to aluminum stubs with Ag paint, coated with a thin film (20 nm) of Au-Pd alloy, and examined with a JEOL JSM-25 II electron microscope. The bulk mineralogy of each layer and certain zones within each layer were determined from randomly oriented powder mounts using a Philips X-ray diffractometer and monochromatic CuK$\alpha$ radiation.

## RESULTS AND INTERPRETATION

### *Stratigraphic-mineralogic relationships*

The bulk mineralogy of the overburden, underclay, and the partings between the lignite seams (interseams)

https://doi.org/10.1346/CCMN.1987.0350405 Published online by Cambridge University Press

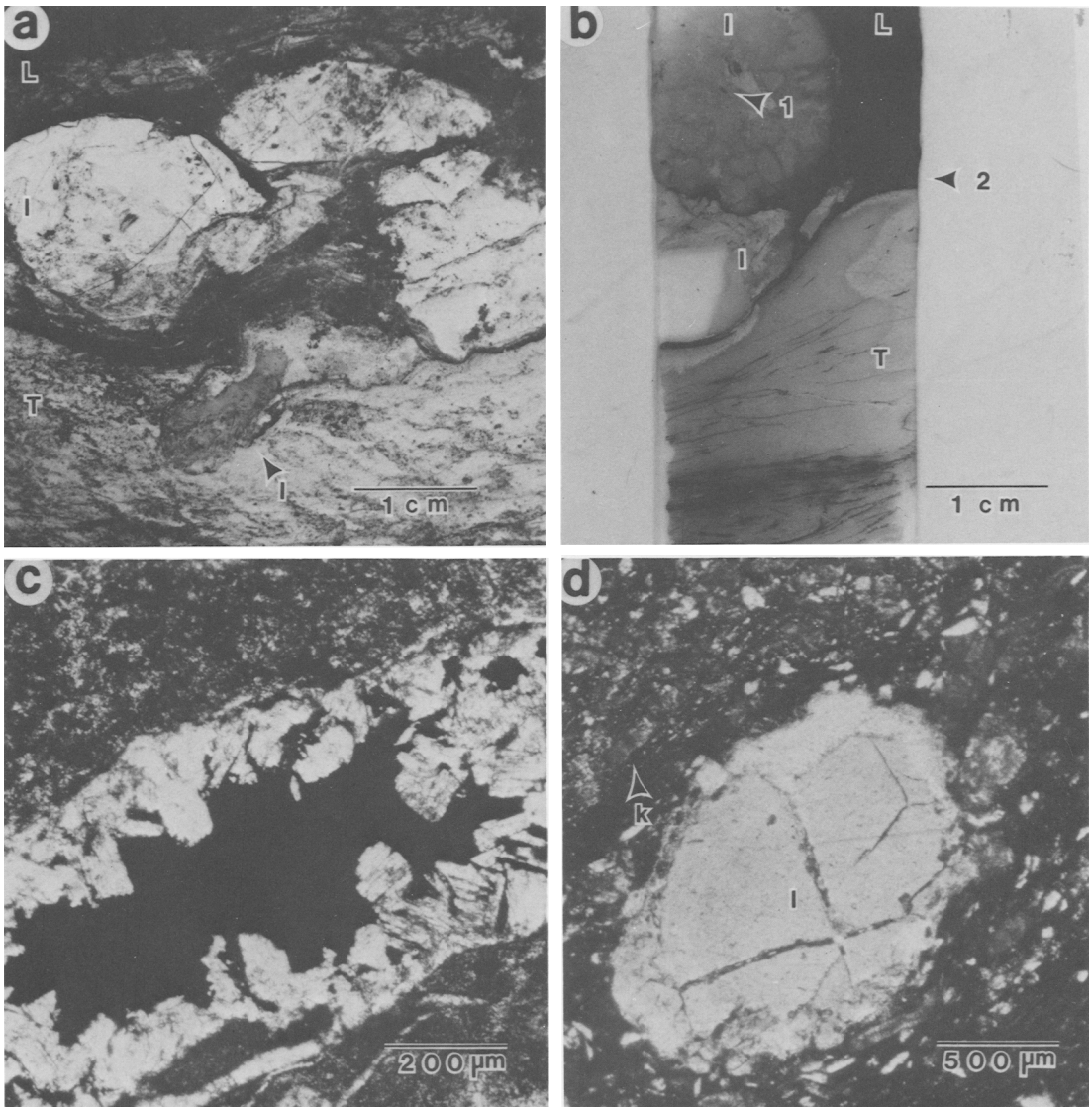


Figure 5. Photographs (a) and (b) showing large (> 1 cm) subrounded inclusions (I) within kaolinized volcanic layers (T). A smaller (< 1 mm) volcanic fragment located in the area indicated by arrow 2 in (b) is shown in micrograph (d). Photomicrograph (c) (plane polarized light) shows large crystals of clinoptilolite in a vug near the area indicated by arrow 1 in (b). L = lignite and k = kaolinite particle.

is summarized in Figure 2. The three layers indicated by arrows in Figure 2 contain negligible quartz (Figure 3) and appear to be volcanic in origin based on micromorphological evidence. Optical microscopy data indicate that the morphology, relative abundance, distribution, and size of the quartz grains in the three volcanic strata markedly differ from those in the A-B, B-C, and brown (No. 2) layers, which apparently consist of mixed volcanic and nonvolcanic materials. Figure 4 shows the transition from partially kaolinized volcanic materials (below the dotted line) to the associated nonvolcanic layer containing much larger and subrounded grains of quartz. Quartz is much less abundant in the kaolinized zone, and the quartz grains are much smaller, relatively uniform in size, angular, and evenly distributed (Figure 4b). The presence of pseudomorphs of volcanic glass shards in these strata (Figure 4c) supports a volcanic origin.

At least three major ash falls (represented by the underclay, the C-D interseam, and the white layer) occurred in this swamp. Each of these volcanic episodes was followed by a period of relative stability

https://doi.org/10.1346/CCMN.1987.0350405 Published online by Cambridge University Press

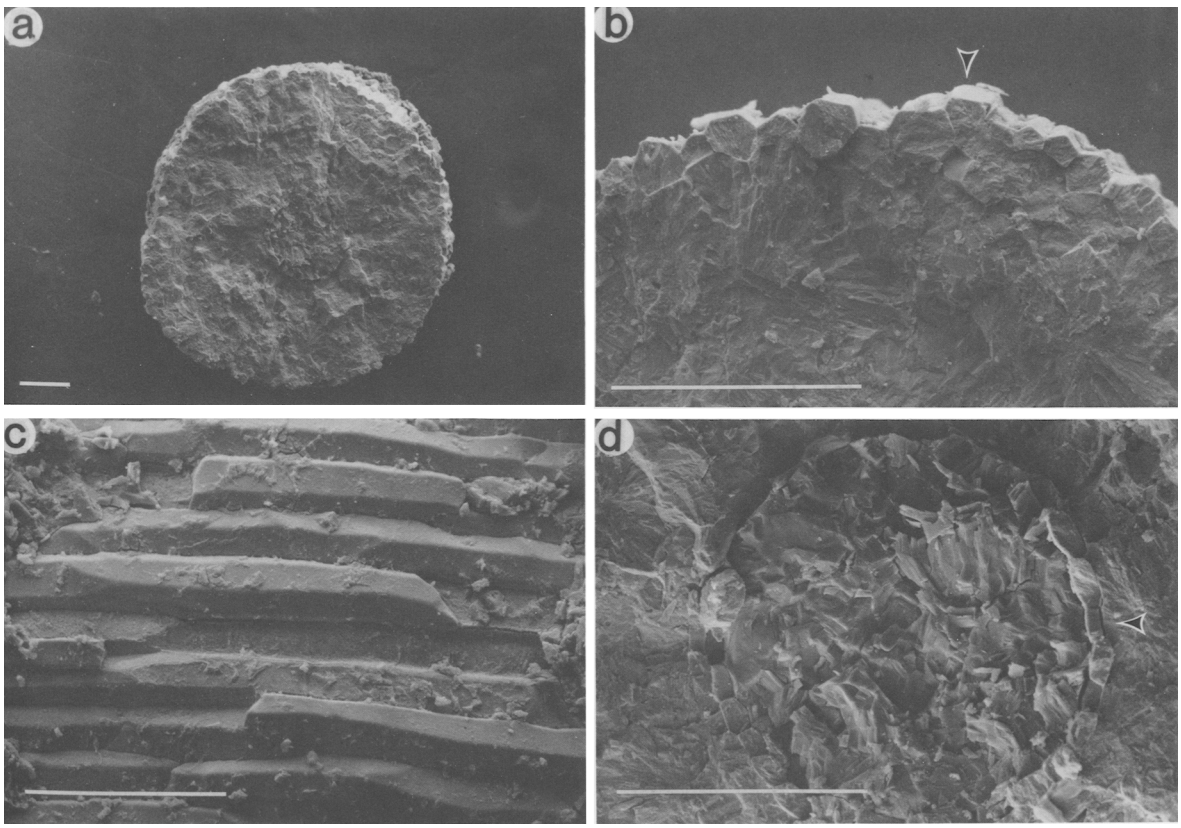


Figure 6. Scanning electron micrographs showing: (a) cross section of a fossil root (from lignite seam A) which is completely impregnated with marcasite; (b) ring of epidermal cells (arrow) around the root; (c) surface morphology of the epidermal cells; and (d) inner ring of cells (arrow) around the vascular cylinder. Each bar represents 100 μm.

during which accumulation of organic matter resumed. The volcanic materials were also subjected to various degrees of *in situ* acid leaching and kaolinization during this period. The underclay is the most kaolinized of the three layers and contains the most kaolinite (inferred from the intensity of kaolinite peaks in Figure 3). The kaolinite shows a well-developed, simple lamellar and vermicular morphology (Figures 4a and 4b), which suggests that it formed in place. Numerous small lenses or blebs (ranging from a few millimeters to several centimeters across) of less kaolinized volcanic material (containing mainly smectite and poorly crystalline kaolinite) occur as inclusions within the kaolinized volcanic layers (Figures 5a, 5b, and 5d). These subrounded inclusions appear to have been incorporated in a soft kaolinized mass before consolidation. They contain large crystals of clinoptilolite in veinlets and vugs (Figure 5c). Numerous microfolds and faults are associated with these inclusions (Figure 5a). The organic matter in the kaolinized zone (Figure 5b) consists of thin layers or laminations which are commonly convoluted and contorted. These laminations of organic matter form microfolds around some of the large kaolinite aggregates suggesting that many of the kaolinite aggregates formed very early, probably before burial and consolidation.

The youngest volcanic ash fall is represented by the white layer above seam A (Figure 2). Apparently, the volcanic ash in this layer had insufficient time to weather appreciably and form kaolinite. This bed consists chiefly of clinoptilolite (Figure 3), which was reported by Pevear *et al.* (1980) to be the initial alteration product of volcanic ash where it is subjected to minimal weathering and leaching. Pseudomorphs of volcanic glass shards (Figure 4c) are abundant in this layer. Deposition of the coarse, micaceous sediments (the uppermost green layer in Figure 2) in the swamp marked the end of the lignite interval at this deposit.

### *Mineralogy of fossilized roots*

Numerous fossil roots, 0.5 to several millimeters in diameter and as long as several centimeters, occur particularly in the strata underlying the white volcanic layer (Figure 2). Most of the roots were preserved in

https://doi.org/10.1346/CCMN.1987.0350405 Published online by Cambridge University Press

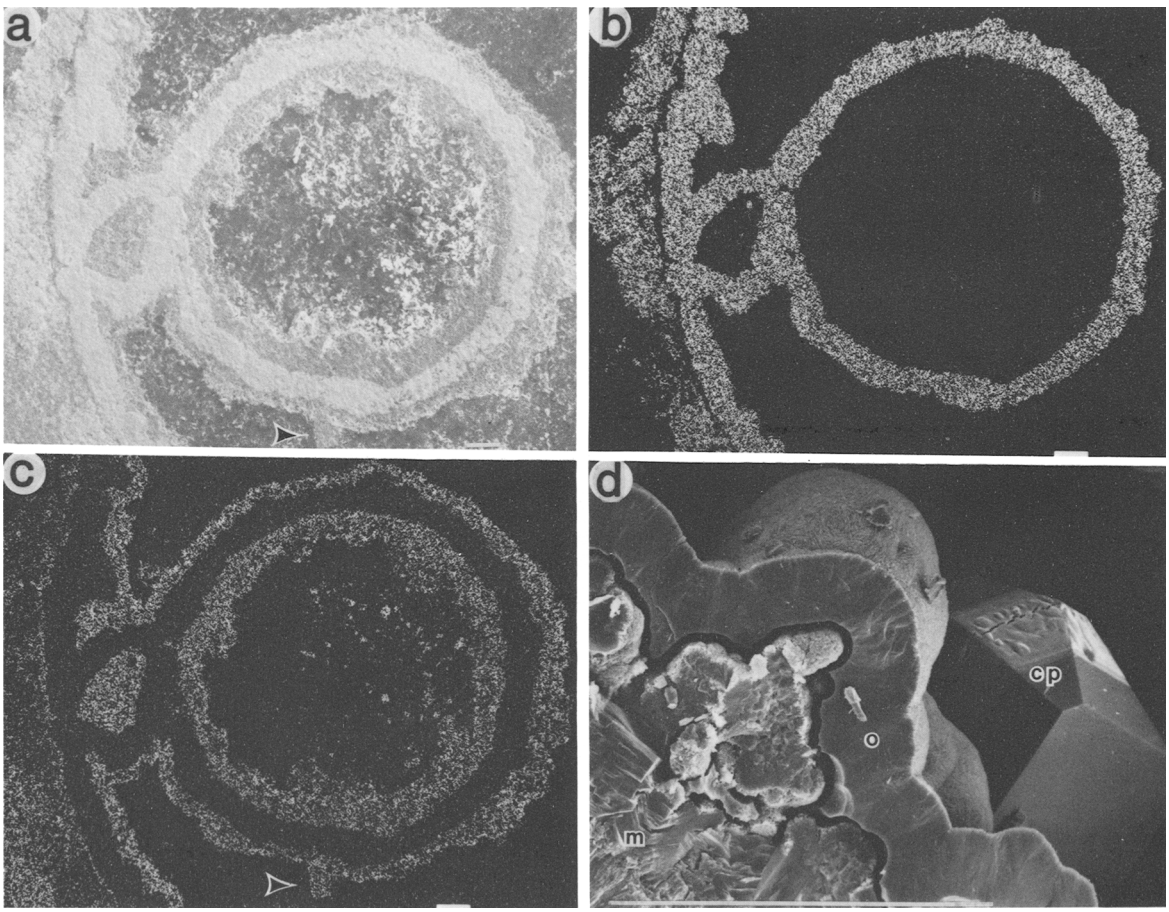


Figure 7. Clinoptilolite, opal-CT, and marcasite in a fossilized root from the brown (No. 2) layer. (a) Scanning electron micrograph of the inner ring of marcasite enclosed by concentric rings of opal-CT and clinoptilolite (arrow). (b) Electron microprobe dot map of S showing the distribution of marcasite. (c) Electron microprobe dot map of Si showing the distribution of opal-CT and clinoptilolite. (d) Scanning electron micrograph showing the relationship between the marcasite (m), clinoptilolite (Cp), and opal-CT (o) within the fossil root shown in a, b, and c. Each bar represents 100 $\mu$m.

their original vertical position and are partially or completely replaced by either marcasite or pyrite, clinoptilolite, and opal-CT, as determined from XRD and electron microprobe data. Although the fossil root shown in Figure 6 is completely filled with marcasite, it is devoid of cellular morphology except for the two ring structures. The lack of cellular details in this root suggests that the softer tissue between the two rings had already decomposed before it was impregnated by marcasite. In some of the fossil roots, the space enclosed by the two rings has been partly or completely filled by Si-rich minerals (opal-CT and clinoptilolite) instead of marcasite (Figure 7). The inner marcasite ring of the root shown in Figure 7 is completely enclosed by concentric rings of opal-CT and clinoptilolite. Clear, euhedral clinoptilolite (such as that shown by arrow in Figures 7a and 7c) can be seen (under a low-power optical microscope) protruding into the open space on the outside of this ring. Details of the contact between the marcasite and the opal-CT are shown in Figure 7d. The opal-CT appears to have precipitated directly on the marcasite. It forms a thin continuous layer (about 20 $\mu$m thick) between marcasite and the clinoptilolite. The opal-CT is distinguishable from marcasite and clinoptilolite based on energy dispersive spectroscopy data (Figure 8) and its characteristic globular morphology (Figures 9a and 9b). The average Si/Al ratio of the clinoptilolite (determined on several crystals) is 4.8, which is in the expected range (4.25–5.25) for this mineral (Boles, 1972).

Crystals of clinoptilolite appear to have grown on and around spherical or globular bodies of opal-CT (Figure 9a). Inclusions of opal-CT were recognized in one large crystal of clinoptilolite (Figure 9b). Many of the clinoptilolite crystals in the fossilized roots show a well-developed "coffin-shape" morphology (Figure 9a), characteristic of clinoptilolite-group minerals (Mumpton and Ormsby, 1976). This clinoptilolite appears

https://doi.org/10.1346/CCMN.1987.0350405 Published online by Cambridge University Press

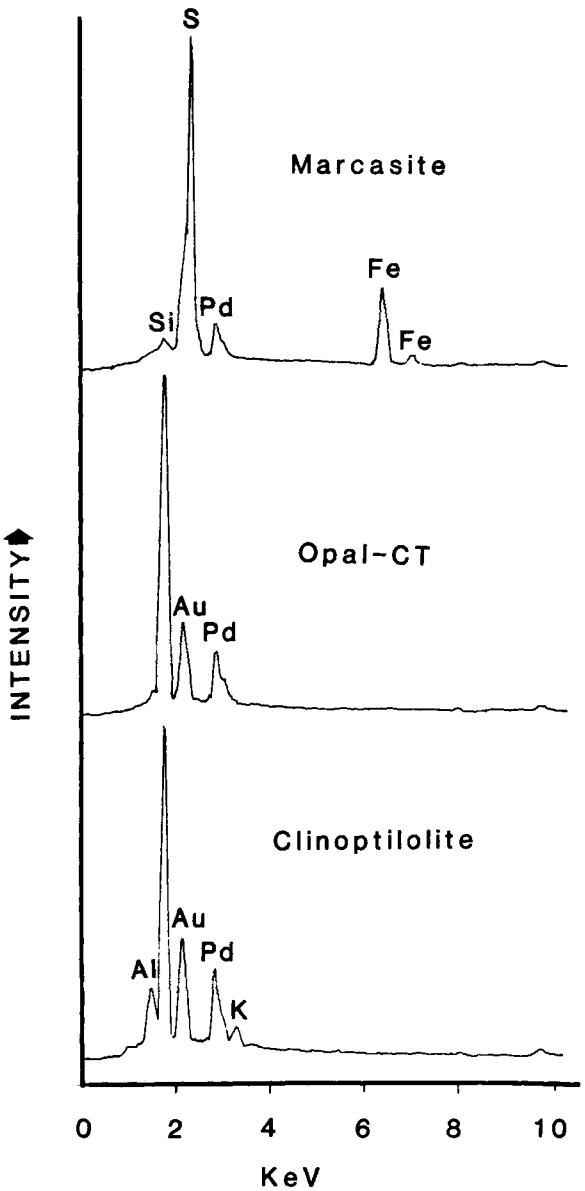


Figure 8. Energy dispersive X-ray spectra of the marcasite, opal-CT, and clinoptilolite zones shown in Figure 7d.

banded or zoned, and the lighter bands apparently formed by dewatering of the zeolite under the electron beam. The banding is apparently controlled by cleavage.

*Minerals in fractures and veinlets*

Numerous vertical and horizontal fractures and veinlets filled with crystals of clinoptilolite and pyrite (Figure 9c) occur in the lignite seams and the associated strata. The origin of these fractures is not clearly understood, although Snedden (1979) suggested that they were formed during periodic exposure to drying conditions. Such an origin may explain some of the frac-

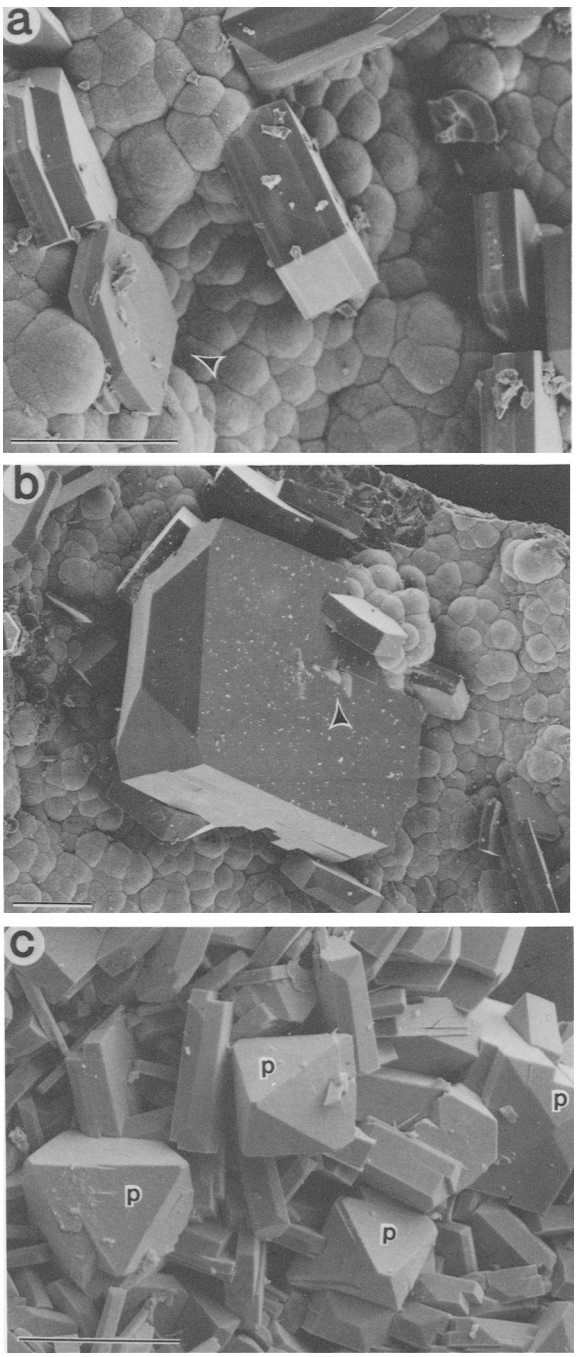


Figure 9. Scanning electron micrographs showing: (a) euhedral, apparently zoned crystals of clinoptilolite having coffin-shape morphology (arrow) and globular lepispheres of opal-CT in a fossil root (from brown layer No. 2); (b) inclusions of opal-CT (arrow) within a clinoptilolite crystal; and (c) interpenetration of pyrite octahedra (p) and clinoptilolite crystals in a vein from lignite seam C. Each bar represents 100 $\mu$m.

https://doi.org/10.1346/CCMN.1987.0350405 Published online by Cambridge University Press

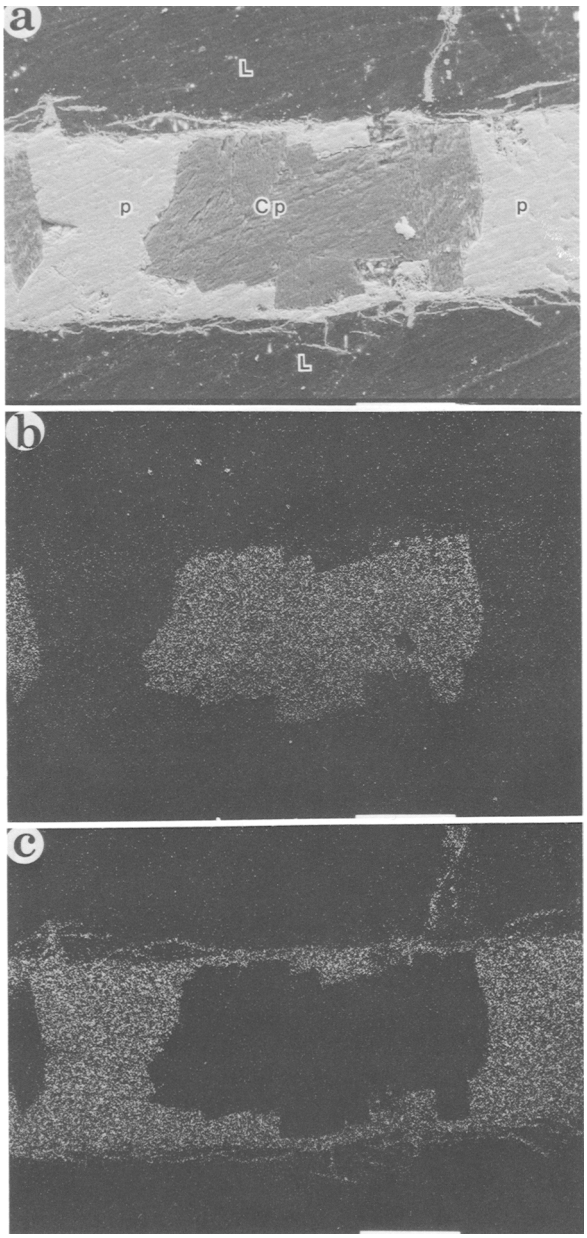


Figure 10. Photomicrographs showing clinoptilolite-pyrite association in a veinlet in lignite (L) seam D: (a) crystals of clinoptilolite (Cp) enclosed by pyrite (p); (b) electron microprobe dot map of Si showing the location of clinoptilolite; and (c) electron microprobe dot map of S showing the location of pyrite. Each bar represents 100 μm.

tures in the non-lignitic strata, but many fractures in the lignite may have formed by differential compaction of the partially decomposed organic materials after burial. These fractures are particularly common in lignite seams A and D and also in the brown layer (No. 2) underlying the white volcanic layer (Figure 2). Many of the veinlets and fractures contain large crystals of clinoptilolite (Figure 9c). The clinoptilolite crystals

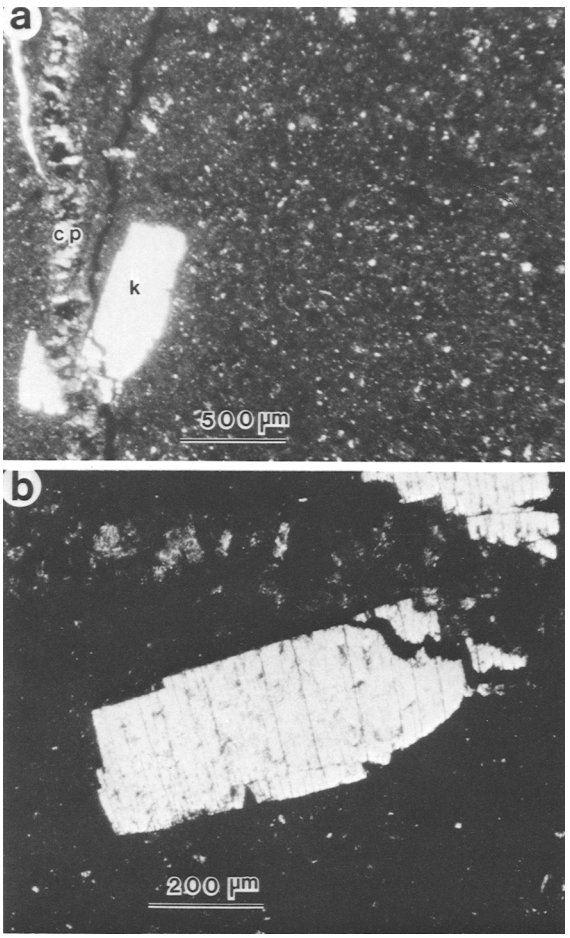


Figure 11. Photomicrographs (crossed polars) showing: (a) a veinlet of clinoptilolite (Cp) that cuts across a detrital kaolinite (k) particle; and (b) the characteristic basal cleavage of the kaolinite particle shown in (a).

within these fractures and veinlets are less well developed morphologically than those in the fossilized roots and show much interpenetration with each other and with many of the associated pyrite octahedra (Figure 9c). The clinoptilolite crystals shown in Figure 10 are completely enclosed by pyrite which apparently precipitated from iron-bearing solutions during later stages of the coalification process. The clinoptilolite veinlet shown in Figure 11 cuts across an apparently detrital aggregate of kaolinite. A detrital origin is postulated for this kaolinite because it is a lone grain in a non-kaolinized groundmass of very fine grained clinoptilolite in the transitional zone between the white layer (Figure 2) and the underlying brown layer (No. 2). The brown layer (No. 2) consists of mixed or reworked volcanic and non-volcanic materials.

## DISCUSSION

The apparently metastable mineral assemblage of opal-CT + clinoptilolite + kaolinite in many of the

https://doi.org/10.1346/CCMN.1987.0350405 Published online by Cambridge University Press

strata investigated suggests that these strata were subjected to at least several cycles of alteration processes including: *in situ* acid weathering in a Late Eocene swamp (which resulted in formation of kaolinite) and a later resilication of the partially kaolinized material after burial. The latter process resulted in the precipitation of the opal-CT and clinoptilolite in the fossilized roots and in fractures in the lignite and the partially kaolinized strata.

The blebs or inclusions of less kaolinized volcanic material in kaolinized volcanic layers appear to have been incorporated into a soft, partially kaolinized mass before burial. The mechanism by which these subrounded inclusions were emplaced within the kaolinized layers is, however, not well understood. Inasmuch as pseudomorphs of vitric shards were observed in these inclusions, they probably are not volcanic bombs (D. R. Pevear, Exxon Production Research Company, P.O. Box 2189, Houston, Texas 77001, personal communication). Local erosional and depositional processes associated with overbank flooding might have produced these inclusions. Such processes also probably resulted in the disruption and transportation of some of the kaolinite aggregates or crystallites. The kaolinite particle shown in Figure 11 probably was transported and deposited in a matrix of fine-grained material consisting of altered volcanic ash. It was later split into two parts, possibly as a result of drying and cracking of the sediment. The large crystals of clinoptilolite within this crack or veinlet and those in fractures in the volcanic inclusion shown in Figure 5c were formed later, probably after burial.

Such a resilication process may also explain the coexistence of marcasite, clinoptilolite, and opal-CT in the fossilized plant roots, and pyrite with clinoptilolite in fractures and veinlets in lignite. According to Edward and Baker (1951), a reducing environment and a slightly acidic pH are required for precipitation of marcasite, whereas clinoptilolite forms in slightly alkaline conditions (Grim and Güven, 1978). Thus, marcasite probably precipitated in the partially decomposed roots before or soon after burial when the conditions were acid and reducing. The initial influx of Si-rich solutions into the fossil roots resulted in precipitation of opal-CT that forms thin layers or coatings on the marcasite (Figure 7d). These layers are clearly visible in thin sections. A change in the chemical microenvironment or the pH within or outside the partially decomposed roots might have initiated the change from precipitation of opal-CT to precipitation of clinoptilolite. The clinoptilolite crystals precipitated directly on the opal-CT lepispheres, and some of these crystals contain inclusions of opal-CT (Figure 9b). Precipitation of large crystals of clinoptilolite in the fossil roots and in veinlets and fractures in the lignite and partially kaolinized strata apparently resulted from redistribution of Si-rich solutions after burial. A similar process was proposed to explain the presence of clinoptilolite in the kaolinitic tonstein layers investigated by Senkayi *et al.* (1984). The siliceous minerals (opal-CT and clinoptilolite) completely enclose marcasite in the fossil roots (Figure 7), whereas pyrite encloses clinoptilolite in the fractures within lignite. This suggests that the marcasite formed before the resilication process, whereas pyrite formed much later.

Although marcasite is common in plant remains within lignite (Brinkmann, 1977), coexistence of clinoptilolite and marcasite has not been previously reported; however, an unusual occurrence of well-developed crystals of heulandite, as long as 4 mm, in fossil wood from the Denver Formation of Colorado was reported by Modreski *et al.* (1983). Modreski *et al.* (1983) employed the heating treatment described by Mumpton (1960) rather than the Si/Al ratios used in the present study to identify the heulandite. According to Modreski *et al.* (1983) alteration of volcanic glass in the Denver Formation released Si and other soluble ions into the ground water. The heulandite in plant structures precipitated from these Si-rich solutions. Similar processes probably resulted in the crystallization of opal-CT and clinoptilolite within the fossil roots investigated in this study. The relatively extensive space available for crystal growth allowed crystallization of extremely large zeolite crystals in the fossil roots of our study and in the petrified wood studied by Modreski *et al.* (1983).

## ACKNOWLEDGMENTS

This research was partially supported by the Center for Energy and Mineral Resources, Texas A&M University. We thank J. M. Ehrmann for his help with the electron microprobe work. We also acknowledge the San Miguel Electric Cooperative for allowing us to obtain samples from their property. Acknowledgments are due J. J. Doolittle and G. Camber for helping with the sampling. The authors appreciate the suggestions of F. A. Mumpton, W. R. Reynolds, R. A. Sheppard, and D. R. Pevear. We are grateful to the micromorphology group in the Soil Science Department at Texas A&M University, especially R. Drees, for the opportunity to use their equipment and facilities.

## REFERENCES

Boles, J. R. (1972) Composition, optical properties, cell dimensions, and thermal stability of some heulandite group zeolites: *Amer. Miner.* **57,** 1463–1493.

Brinkmann, K. (1977) Mineralogy and geochemistry of iron sulfides in the overburden of the Frechen open cast mine (Rhenish soft coal field): *Neues Jahrb. Mineral. Abh.* **129,** 333–352.

Edward, A. B. and Baker, G. (1951) Some occurrences of supergene iron sulfides in relation to their environment of deposition: *J. Sediment. Petrol.* **21,** 34–46.

Grim, R. E. and Güven, N. (1978) *Bentonites:* Elsevier, Amsterdam, 256 pp.

Henderson, J. H., Jackson, M. L., Syers, J. K., Clayton, R. N., and Rex, R. W. (1971) Cristobalite authigenic origin in relation to montmorillonite and quartz origin in bentonites: *Clays & Clay Minerals* **19,** 229–238.

Kaiser, W. R. (1985) Texas lignite-status and outlook to 2000: *Texas Bur. Econ. Geol. Circ.* **76,** 17 pp.

McNulty, J. E. (1978) Geology of the San Miguel lignite deposit: *Proc. Gulf Coast Lignite Conf. on Geology, Utilization and Environmental Aspects,* W. R. Kaiser, ed., *Texas Bur. Econ. Geol. Rept. Inv.* **90,** 79–83.

Ming, D. W. and J. B. Dixon (1986) Clinoptilolite in south Texas soils: *Soil Sci. Soc. Amer. J.* **50,** 1618–1622.

Modreski, P. J., Verbeek, E. R., and Grout, M. A. (1983) Zeolites replacing plant fossils in the Denver Formation, Lakewood, Colorado: *Rocks Miner.* **59,** 18–28.

Mumpton, F. A. (1960) Clinoptiloite redefined. *Amer. Miner.* **45,** 351–369.

Mumpton, F. A. and Ormsby, W. C. (1976) Morphology of zeolites in sedimentary rocks by scanning electron microscopy: *Clays & Clay Minerals* **24,** 1–23.

Pevear, D. R., Williams, V. E., and Mustoe, G. E. (1980) Kaolinite, smectite, and K-rectorite in bentonites: Relation to coal rank at Tulameen, British Columbia: *Clays & Clay Minerals* **28,** 241–254.

Reynolds, R. C., Jr. and Anderson, D. M. (1967) Cristobalite and clinoptilolite in bentonite beds of the Colville Group, northern Alaska: *J. Sediment. Petrology* **37,** 966–969.

Reynolds, W. R. (1970) Mineralogy and stratigraphy of Lower Tertiary clays and claystones of Alabama: *J. Sediment. Petrology* **40,** 829–838.

Senkayi, A. L., Dixon, J. B., Hossner, L. R., Abder-Ruhman, M., and Fanning, D. S. (1984) Mineralogy and genetic relationships of tonstein, bentonite, and lignitic strata in the Eocene Yegua Formation of east-central Texas: *Clays & Clay Minerals* **32,** 259–271.

Snedden, J. W. (1979) Stratigraphy and environment of deposition of the San Miguel lignite deposit, northern McMullen and southeastern Atascosa Counties, Texas: M.S. thesis, Texas A&M University, College Station, Texas, 161 pp.

*(Received 17 February 1986; accepted 30 September 1986; Ms. 1561)*